JOURNAL OF GEOPHYSICAL RESEARCH, VOL. 104, NO. D23, PAGES 30,445–30,462, DECEMBER 20, 1999

A textbook example of long-range transport: Simultaneous observation of ozone maxima of stratospheric and North American origin in the free troposphere over Europe

Andreas Stohl

Lehrstuhl für Bioklimatologie und Immissionsforschung, University of Munich, Freising, Germany

Thomas Trickl

Fraunhofer-Institut für Atmosphärische Umweltforschung, Garmisch-Partenkirchen, Germany

Abstract. We describe an episode of a stratospheric intrusion into the free troposphere over Europe followed by a long-range transport of ozone from the North American boundary layer. Observational data showed the presence of a thin tongue of stratospheric air in the free troposphere for at least 36 hours. This filament was found in data from two ozone soundings and was recorded continuously for 26 hours by a high-resolution ozone lidar. The stratospheric air also intercepted two high Alpine summits, causing elevated ozone and beryllium 7 concentrations. Trajectory, particle dispersion model, and potential vorticity analyses confirmed the stratospheric nature of the tongue. In the lidar data, following the intrusion, pockets of elevated ozone concentrations (80–100 ppb) were found in the free troposphere close to the tropopause. The low potential vorticity values and high water vapor content in these ozone-rich pockets and trajectory analyses suggest that the ozone was photochemically produced in the boundary layer over eastern North America, followed by rapid uplifting in a warm conveyor belt over the Atlantic Ocean ahead of a frontal system. This was confirmed by ozone and water vapor measurements aboard commercial airliners crossing the warm conveyor belt. The air mass trajectories in both the stratospheric intrusion and the warm conveyor belt were tightly bundled, emphasizing the importance of the coherency of airstreams for long-range ozone transport.

1. Introduction

Ozone (O_3) can be produced by tropospheric in situ photochemistry locally or regionally, but owing to its long photochemical lifetime of the order of 1–2 months [*Liu et al*., 1987], it can also be advected over long distances from a source region. Of special importance are transport phenomena which are coherent in a Lagrangian framework, thus preventing the O_3 (or any other species with enhanced concentrations) to be diluted by mixing with the surrounding air. In the extratropics, such coherent airstreams are related to synoptic weather systems. For instance, the pseudo-Lagrangian conveyor belt model [*Carlson*, 1980; *Browning*, 1990; *Browning and Roberts*, 1994, 1996] describes three characteristic streams in a coordinate system moving with a synoptic system: the warm conveyor belt (WCB), the cold conveyor belt, and the dry intrusion. The WCB is an ascending airstream at the leading edge of a trough [*Browning*, 1999], the cold conveyor belt is an airflow ahead of a surface warm front, and the dry intrusion is a descending airstream related to tropopause folding [*Browning*, 1997]. It is not yet known how coherent these airstreams are compared to others. However, *Wernli and Davies* [1997] and *Wernli* [1997] explored their Lagrangian characteristics and found that especially the WCB and the dry intrusion are associated with coherent ensembles of trajectories (CETs) exhibiting strong vertical motions. *Cohen and Kreitzberg* [1997] have shown that the boundaries between these airstreams, which are usually close to the air mass fronts, are much less coherent. *Bethan et al*. [1998] recently demonstrated the capacity of the above airstreams for causing strong gradients in trace gas concentrations near fronts. In this paper, on the basis of the example of a single episode, we explore the significance of these airstreams for long-range O_3 transport.

Mixing across the tropopause and diabatic cooling in the tropopause region can cause stratospheric air to get irreversibly transported into the troposphere [*Holton et al*., 1995]. Stratospheric intrusions are important for the chemistry of the troposphere, since their O_3 input is significant as compared with in situ photochemical production [*Beekmann et al*., 1997; *Roelofs and Lelieveld*, 1997]. In the extratropics this is related to rather small-scale phenomena such as tropopause folds [*Danielsen*, 1968], cutoff lows [*Vaughan*, 1988], thunderstorms [*Poulida et al*., 1996], and gravity wave breaking [*Lamarque et al*., 1996]. Stratospheric intrusions related to upper level frontogenesis occur with the airstreams denoted above as dry intrusions, which can be identified sometimes in water vapor satellite images as dry streamers [*Appenzeller and Davies*, 1992].

Analyses of continuous meteorological and chemical measurements at the Zugspitze peak at a height of 2962 m above sea level (asl) showed that a strong stratospheric influence is present ~5–6% of the time [*Scheel et al*., 1999]. In good agreement with the measurements, frequent, but short episodes of

Paper number 1999JD900803.
0148-0227/99/1999JD900803$09.00

direct stratospheric intrusions with very strong impact were also found in the results of a continuous 3-year simulation with a tracer model [*Stohl et al*., 1999], which was also used for the present study. These episodes are usually related to coherent airstreams from the stratosphere. Owing to the impact of these events, the O_3 concentration in the free troposphere over Europe exhibits a maximum in late winter and a deep minimum in summer [*Stohl et al*., 1999]. Occasionally, these descending airstreams may proceed to the ground and cause the surface O_3 concentrations to increase [*Davies and Schuepbach*, 1994; *Eisele et al*., 1999; *Stohl et al*., 1999]. A quasi-continuous, but highly variable stratospheric background influence at a level of ~700 hPa not associated with direct dry intrusions was also identified in model simulations [*Stohl et al*., 1999]. This background influence is related to the outflow of stratospheric intrusions, which appears to be much less coherent than the intrusion itself. O_3 and other stratospheric tracers contained in this outflow get mixed with the surrounding tropospheric air, and the stratospheric character of the air mass gets lost with time. Obviously, such indirect intrusions are very difficult to detect in measurement data.

This paper describes an episode during which stratospheric air was coherently transported deep into the troposphere over Europe within a dry intrusion. The episode is not described here because it was an extraordinarily strong event; deeper intrusions than the one described here were documented, for instance, by *Stohl et al*. [1999]. However, for this episode the subsidence of the stratospheric air into the troposphere was particularly well documented with ozone-lidar and other measurements. Furthermore, the stratospheric intrusion was accompanied by another coherent long-range transport of O_3 within a WCB. We show evidence that elevated O_3 concentrations in the outflow of this WCB, found above the air intruded from the stratosphere and associated with high water vapor concentrations and very low values of potential vorticity, had their source in the North American boundary layer at the time of a photochemical O_3 episode.

Parrish et al. [1993] have shown that O_3 concentrations within the continental outflow from North America can be strongly enhanced. This anthropogenic O_3 can be detected quite easily at islands close to the American east coast [*Parrish et al*., 1998]. Although its detection gets more difficult as one proceeds eastward over the Atlantic Ocean, *Parrish et al*. [1998] also reported a clear anthropogenic influence at 1-km height over the Azores in the middle of the Atlantic Ocean. However, using data from the west coast of Ireland, *Derwent et al*. [1998] found only weak, if any, influence from North American sources. For more passive tracer gases than O_3, though, occasional pollution from North America has been reported for the same site. *Jennings et al*. [1996] found an episode of enhanced CO concentrations, and *Ryall et al*. [1998] presented evidence for a weak influence on the concentrations of inert chlorofluorocarbons. *Ryall et al*. [1998] also discussed the importance of the absence of chaotic advection [*Ottino*, 1989; *Pudykiewicz and Koziol*, 1998] to prevent dilution of the North American air mass in order to allow its detection in measurement data. Transport within a WCB clearly fulfills this requirement.

This paper is organized as follows: In section 2 we introduce the observational data and the modeling tools. In section 3 we describe the synoptic situation and introduce the two coherent airflows which are the subject of this study. In section 4 we interpret station, ozone sonde, lidar, and aircraft observations and relate them to the dry intrusion and the WCB using backward trajectories and particle model simulations. In section 5, we draw some conclusions.

2. Data and Models

2.1. Measurement Data

This study was motivated by hourly differential-absorption lidar measurements of O_3 made in Garmisch-Partenkirchen (11.06°E, 47.5°N, 740 m asl) between May 28, 1997, at 1500 UTC and May 29, 1997, at 1700 UTC. The range of these measurements was from 150 m above the ground to ~5 km above the tropopause, and their vertical resolution was between 50 m at lower levels and ~500 m near the tropopause and was thus suitable for detecting narrow laminae in the O_3 concentrations. The accuracy was of the order of 3 ppb in the troposphere. A more complete description of these measurements is given by *Eisele et al*. [1999].

Ten hours before the lidar measurements started, an ozonesonde was launched at the Hohenpeissenberg observatory (11.02°E, 47.80°N), just 40 km north of the lidar site. The Hohenpeissenberg data were recently described, for instance, by *Steinbrecht et al*. [1998]. Another ozonesonde ascent took place at Payerne (6.95°E, 46.82°N), some 350 km to the west of the lidar site. These soundings have the advantage of providing meteorological data in addition to O_3. Of special interest are the humidity measurements, since stratospheric air masses are much drier than tropospheric ones. In addition, operational radio-sounding data from several sites were used.

High mountain peaks provide a unique opportunity for continuous monitoring in free-tropospheric air. We used data from the Zugspitze summit (2962 m asl), just about 10 km southwest of the lidar site, and from the Jungfraujoch observatory in Switzerland (7.98°E, 46.55°N, 3580 m), ~250 km west of the lidar site. At both stations, O_3, meteorological, and other measurements were made. Of special interest in the current context were measurements of beryllium 7 (^{7}Be), a cosmogenic radionuclide with a radioactive decay half-life of 53 days that is formed in the stratosphere and upper troposphere and attaches to aerosols [*Koch and Mann*, 1996]. It is not an unambiguous stratospheric tracer because it is also produced in the troposphere and is removed by wet deposition, but high concentrations of ^{7}Be are nevertheless a valuable indicator for the occurrence of stratospheric intrusions. The time interval of the ^{7}Be measurements was 24 hours at Zugspitze and 48 hours at Jungfraujoch [*Zanis et al*., 1999].

Aircraft measurements, obtained within the Measurement of Ozone and Water Vapor by Airbus In-Service Aircraft (MOZAIC) program [*Marenco et al*., 1998], were used to study O_3 and water vapor concentrations over the remote Atlantic. The precision of the O_3 measurements is better than ±2 ppb [*Marenco et al*., 1998], and the uncertainties in the relative humidity measurements are within ±7% in the upper troposphere and lower stratosphere [*Helten et al*., 1998]. Integrated data with a time resolution of 1 min from approximately five flights per day were available during the period studied. On May 28, three trans-Atlantic flights crossed the WCB mentioned above, but we will concentrate on data from only one flight that departed from Atlanta on May 27 at 2100 UTC and arrived at Frankfurt on May 28 at 0500 UTC.

Supplementary information was obtained from infrared images taken by the advanced very high resolution radiometer (AVHRR) aboard National Oceanic and Atmospheric Administration (NOAA) polar-orbiting satellites in the 11.5–12.5 μm

spectral range; radiance measurements of the Meteosat satellite in the 6-μm water vapor channel; and total column O_3 satellite measurements from the TIROS Operational Vertical Sounder (TOVS).

2.2. Modeling Tools

Two models, both set up on model level data from the *European Centre for Medium-Range Weather Forecasts* (*ECMWF*) [1995] (T213 L31 model), were used to interpret the measurement data. The ECMWF data had a horizontal resolution of 1° and a time resolution of 3 hours (analyses at 0000, 0600, 1200, 1800 UTC; 3-hour forecasts at 0300, 0900, 1500, 2100 UTC). The computational domain was 100°W–50°E, 24°N–81°N.

The first tool used is the trajectory model FLEXTRA [*Stohl et al*., 1995], which has been validated using constant level balloon [*Stohl et al*., 1997; *Stohl and Koffi*, 1998] and manned gas balloon flights [*Baumann and Stohl*, 1997]. With FLEXTRA it is possible to compute several types of kinematic trajectories, for instance, isobaric, isentropic, and three-dimensional trajectories. *Stohl and Seibert* [1998], studying potential vorticity (PV) conservation, have shown that three-dimensional trajectories are more accurate than all other types, including isentropic trajectories. Thus three-dimensional trajectories were used throughout this study, but the impact of the isentropic assumption is demonstrated for one example. In addition to the trajectory positions, FLEXTRA also outputs other information, such as PV, which is interpolated from grid point values.

The second tool used is the Lagrangian particle dispersion model FLEXPART (version 3.0) [*Stohl et al*., 1998; *Stohl and Thomson*, 1999]. This model has been developed to calculate the dispersion of nonreactive tracers. It has recently been validated with data from three large-scale tracer experiments in America and Europe [*Stohl et al*., 1998], and it performed very well in comparison with other models. FLEXPART treats advection and turbulent diffusion of a tracer by calculating the trajectories of a multitude of particles. Stochastic wind fluctuations, obtained by solving Langevin equations for the three wind components, are added to the grid-scale winds interpolated from ECMWF data, which are used to advect the trajectories. The magnitude and the Lagrangian decorrelation times of these fluctuations are obtained from turbulence parameterizations. The concentrations of the tracer are evaluated on a Eulerian grid (resolution 1° × 1° × 250 m) using a kernel method (this is similar to summing up the masses of all particles contained in a grid cell and dividing by its volume).

For this study we simulated the transport of two passive tracers: a stratospheric O_3 tracer and a tracer for North American emissions. The latter was a classical simulation with a Lagrangian particle dispersion model, namely, to describe the dispersion of a tracer released from a low-level source. One million tracer particles were "emitted" at the surface at a constant rate throughout the simulation period (May 21, 0000 UTC to May 31, 1200 UTC) and within the area 95°W–72°W, 34°N–44°N. The absolute value of the emitted mass of this "North America tracer" is irrelevant in the current context, since we will only discuss relative values. The particles arriving in the vertical grid column containing the lidar measurement site were used to calculate the tracer concentrations in the column, which were then compared with the measurement data. Similarly, concentrations were determined at the positions of the MOZAIC aircraft.

The simulation of the stratospheric O_3 tracer required some modifications of FLEXPART, described in detail by *Stohl et al*. [1999], who used this model version for case studies and a 3-year continuous simulation. Particles were not released from a source within the model domain. Instead, 3.5 million particles were initialized uniformly distributed in the whole model stratosphere on May 26 at 0000 UTC. The tropopause, separating the troposphere and the stratosphere, was assumed to coincide with a surface of 1.6 potential vorticity units (pvu, 1 pvu = 10^{-6} K m^2 kg^{-1} s^{-1}) [*World Meteorological Organization* (*WMO*), 1986]. During the simulation, suitable boundary conditions were applied by continuously generating new particles at the inflowing boundary. The computational domain was somewhat smaller than for the other simulation (50°W–50°E, 24°N–81°N). The mass of each particle was adjusted to achieve a concentration determined with the relationship O_3 [ppb] = C [ppb/pvu] × PV [pvu], with C = 40 ppb/pvu, based on the observation that stratospheric O_3 is highly correlated with PV [e.g., *Danielsen*, 1968]. C was derived from a correlation analysis of Payerne O_3 sounding data available for May 26, 28, and 30 with analyzed PV from ECMWF. Comparing many O_3 profiles from several sites, *Stohl et al*. [1999] found that C = 60–64 ppb/pvu would be more typical for this time of the year (the average values of C vary by approximately a factor of 2 with season), but an application of such values led to a considerable overestimation of the O_3 concentrations in the present case. The O_3 tracer does not react chemically but is deposited at the ground according to a detailed resistance parameterization. As chemical processes are not treated in the model, any structures seen in the model results in the troposphere are due to transport from the stratosphere. Again, results are displayed in the grid column containing the lidar measurement site. (More information and the source codes of both FLEXTRA and FLEXPART can be obtained via the Internet at http://www.forst.uni-muenchen.de/LST/METEOR/stohl/astohl.html.)

3. Synoptic Situation

On May 28, 1997, at 0000 UTC, a low in the 1000-hPa geopotential chart was located over central and eastern Europe (Figure 1). On its backside, ahead of a high centered over Britain, subpolar air proceeded southward, causing widespread rain and snow showers in central Europe. The surface low corresponded to an intense trough at 500 hPa with strong pressure gradients especially on its western flank (Figure 1), associated with a large undulation of the jet stream on the 315 K isentropic surface (Figure 2). The PV was elevated in the region of the 500-hPa trough (Figure 3), and large areas of the 315 K isentropic surface were in the stratosphere.

Over the Atlantic Ocean a low both in the 500-hPa and in the 1000-hPa geopotential chart was located to the south of Greenland (Figure 1). Between this trough and the high over Britain, a flow from the southwest was established that turned anticyclonically north of Britain. This southwesterly flow coincided with a WCB that ascended from the boundary layer in the western Atlantic Ocean to the upper troposphere at the leading edge of the trough. This moist airstream is clearly visible as a cloud band near 25°W stretching north toward Iceland in an infrared satellite image on May 29 at 0800 UTC (Figure 4) and may be classified as a WCB with forward sloping ascent [see *Browning*, 1990; *Browning and Roberts*, 1994,

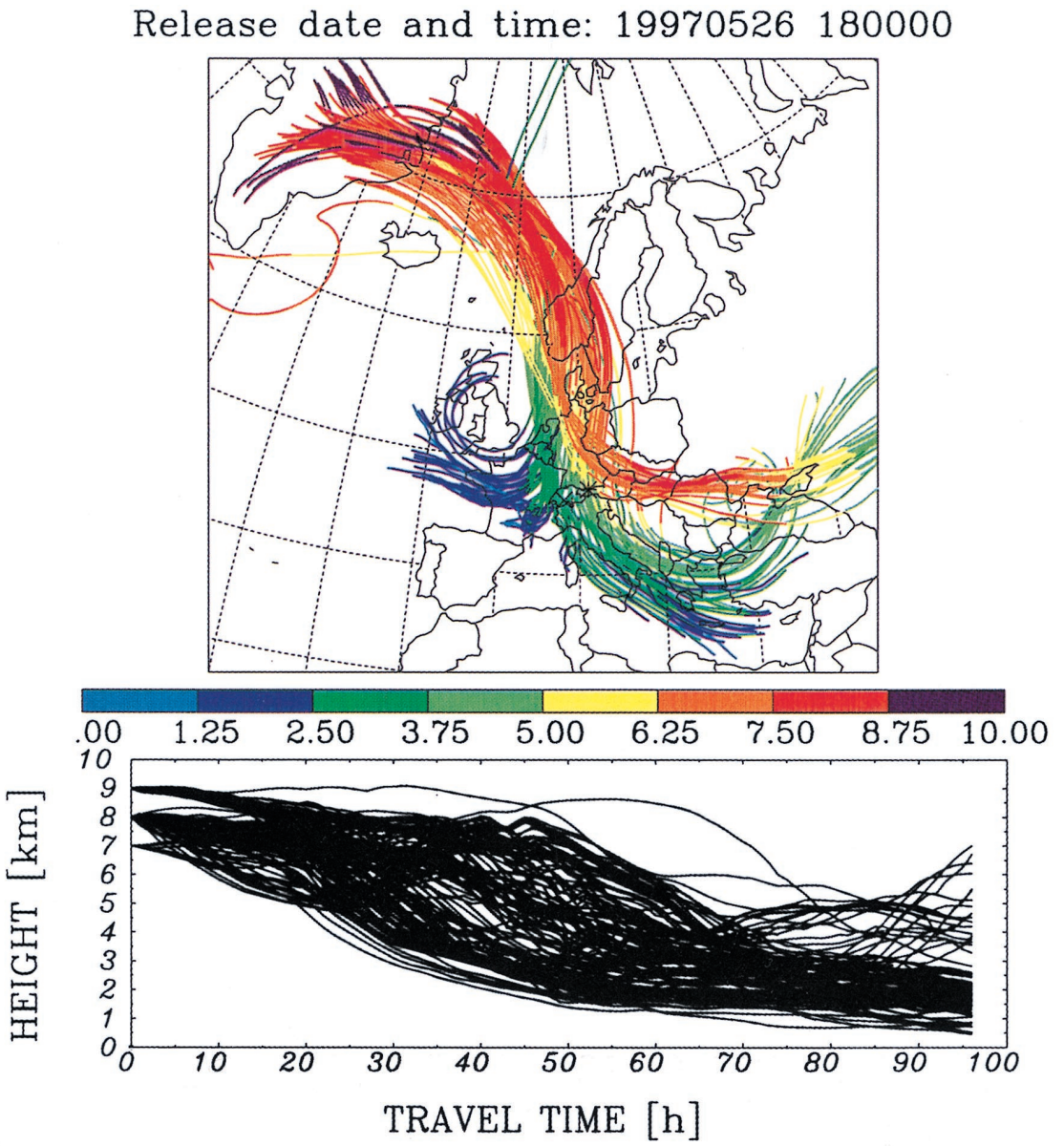

Plate 1. Coherent ensemble of three-dimensional trajectories depicting the intrusion of stratospheric air into the troposphere: (top) The height of the trajectories indicated by the color code. The approximate locations of Hohenpeissenberg, the lidar measurement site, and the Zugspitze summit are denoted by asterisks, the location of Jungfraujoch is denoted by a cross. (bottom) A time-height profile of the trajectories.

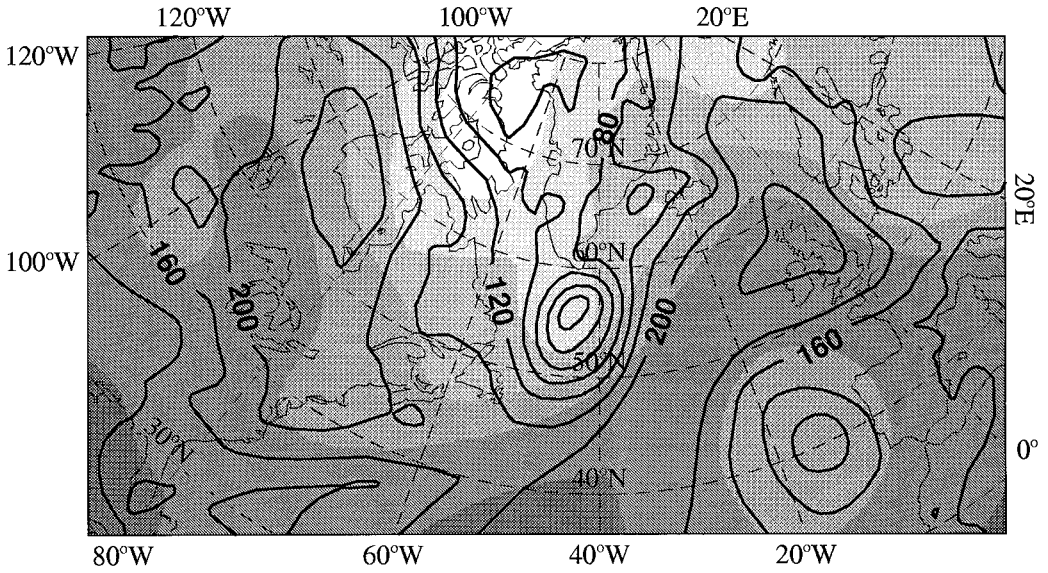

Figure 1. Geopotential at the 500 hPa (shaded every 140 geopotentials dekameters (gpdm) with light shading denoting low values) and the 1000 hPa (isolines every 40 gpdm) surfaces over the northern Atlantic Ocean on May 28, 1997, at 0000 UTC; the plot is based on analysis data from the European Centre for Medium-Range Weather Forecasts (ECMWF).

1996]. Also visible is its outflow that turned southeastward toward Europe.

The WCB can be depicted more clearly using the CET method of *Wernli and Davies* [1997]. For this, we started 60-hour forward trajectories at heights of 100 m and 1000 m above ground level on a grid with 1° spacing in the domain (95°W–10°W, 24°N–70°N) on May 26 at 1800 UTC. To isolate the WCB from other airstreams, we selected those trajectories (a total of 53) from the 8084 calculated trajectories that ascended by at least 8000 m, the typical ascent of a WCB (Figure 5). All selected trajectories were concentrated in a single coherent band connecting the boundary layer at the east coast of North America with the upper free troposphere to the northwest of Europe. The inflow into this conveyor belt to a large part came from the North American continent, whereas the outflow largely affected the troposphere over the European continent. A comparison with the satellite image presented in Figure 4 shows good spatial agreement between the CET and the WCB

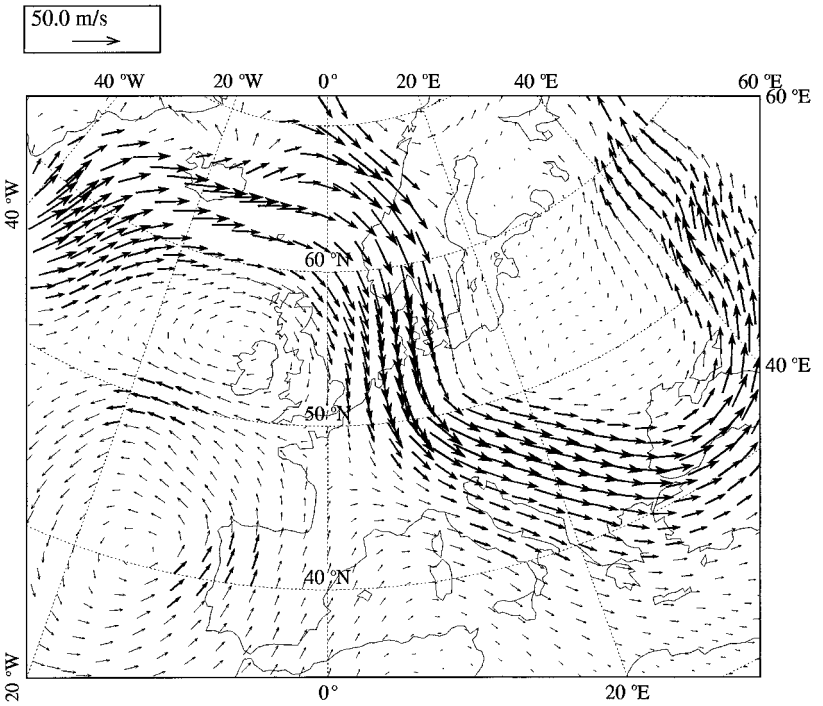

Figure 2. Horizontal wind vectors on the 315 K isentropic surface in the ECMWF analysis for 0000 UTC on May 28, 1997.

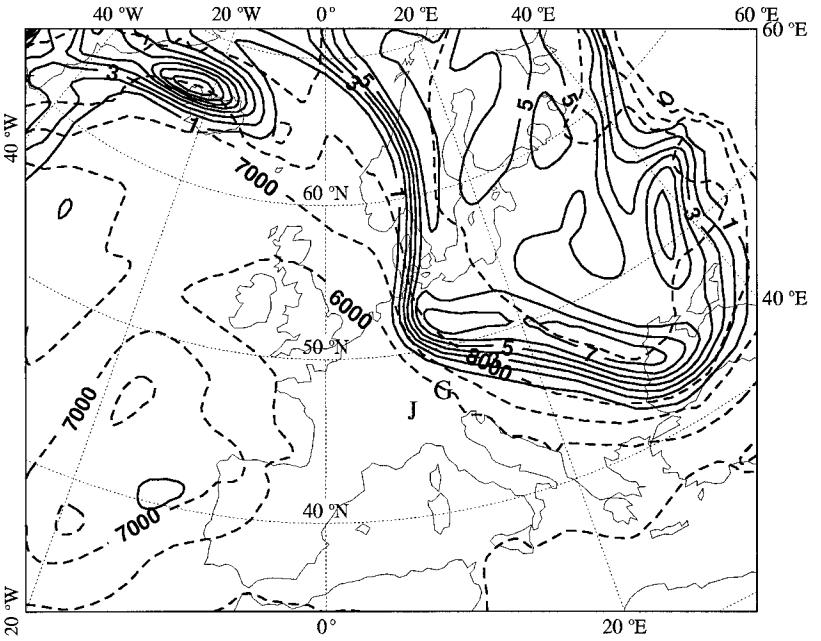

Figure 3. Potential vorticity (solid lines) on the 315 K isentropic surface for 0000 UTC on May 28, 1997; isolines are from 1 to 8 pvu every 1 pvu. Shown in dashed lines is the geopotential of the 315 K surface every 1000 gpdm. G marks the position of the ozone lidar in Garmisch-Partenkirchen; J indicates the location of the Jungfraujoch station.

cloud band, even though the CET is a spatiotemporal entity, whereas the satellite image is instantaneous (and at a later time).

The CET method was also used to depict the pathway of the stratospheric air into the troposphere. We started a large number of three-dimensional forward trajectories at 7000, 8000, 9000, and 10000 m asl in the domain (50°W–10°E, 50°N–80°N) on a 1° × 1° latitude-longitude grid on May 26 at 1800 UTC. Then we selected those that started in the stratosphere (PV > 1.6 pvu) and descended by more than 5000 m (Plate 1). In this way, a CET was obtained that impressively shows the extrusion of stratospheric air over Greenland and its intrusion into the lower troposphere over central and southern Europe. The descent was deeper at the CET's western edge than on its eastern one. The average PV of all CET trajectories decreased from 2.9 pvu at the starting points to 1.7 pvu after 24 hours, 0.8 pvu after 48 hours, and 0.5 pvu after 96 hours.

It is also worthwhile noting that it is imperative to use three-dimensional instead of isentropic trajectories to study stratospheric intrusions, since in the present case, 60% of the CET trajectories experienced a diabatic cooling of >5 K. Diabatic cooling was less effective for the western branch of the CET than for its eastern branch, where cloud processes (and hence also radiative cooling at the cloud tops) were more important. This is in accordance with the studies of *Kowol-Santen* [1998] and *Wirth* [1995] on the role of mixing and diabatic processes in the tropopause region. The CET that was obtained when isentropic instead of three-dimensional trajectories were used contained just a third of the trajectory members of the three-dimensional CET.

The CET corresponded in position to a streamer of dry air revealed in the water vapor images on May 28. This streamer was, however, less distinct than those found during other stratospheric intrusion episodes [*Appenzeller and Davies*, 1992; *Stohl et al*., 1999], which was caused by overrunning moist air from the WCB. Comparing Plate 1 and Figure 5, we see that the outflow of the WCB reached Europe at about the same time as the dry intrusion (on its backside) but at greater heights. At the same time a broad tongue of elevated total column O_3 (400 Dobson units) stretching southwards to central Europe was detected in TOVS satellite measurement data. This was likely caused by three factors: the low tropopause level, the extrusion of O_3 from the stratosphere into the troposphere, and the tropospheric transport of ozone-rich air from North America (as will be shown in section 4).

4. Long-Range Ozone Transport Phenomena

The first observation of the stratospheric air in the troposphere was made by an ozone sonde launched at Hohenpeissenberg on May 28 at 0500 UTC. The observatory was located right in the pathway of the stratospheric air as depicted by the CET (Plate 1). The vertical profile clearly showed an O_3 lamina of 85 ppb just below 6000 m asl (Figure 6) accompanied by low values of relative humidity. These are typical characteristics of stratospheric air as they may be found in ozone sounding data [*Austin and Midgley*, 1994; *Van Haver et al*., 1996].

Another ozonesonde ascent performed at Payerne on May 28 at 1100 UTC yielded a double-peak structure in O_3 with the lower peak at 3500 m (accompanied by relative humidity values of <10%) and the higher one at 7500 m asl (Figure 6). The lower spike is consistent with the CET calculations that showed stratospheric air penetrating deep into the troposphere on the western flank of the intrusion (Plate 1). The origin of the upper peak is not completely clear, especially since there is no correlation between the humidity and the O_3 profiles. However, the model calculations reported later suggest that it may have been caused by the first arrival of air from the North American boundary layer (actually, the model calculations show the arrival of this air mass some 5 hours after the ozone sounding).

Starting from May 28, 1600 UTC, hourly lidar measure-

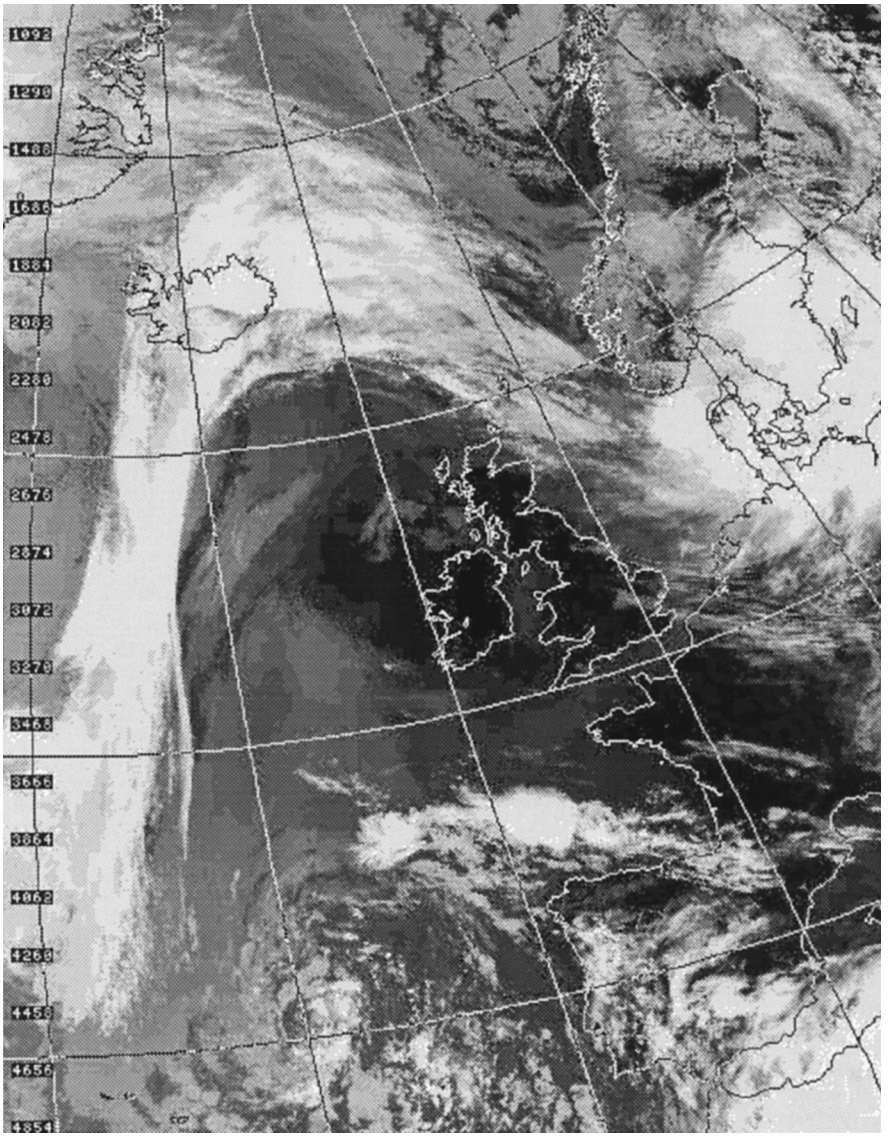

Figure 4. Infrared image taken by the AVHRR aboard the NOAA 12 satellite on May 29, 1997, at 0751 UTC. Image is courtesy of the Dundee Satellite Receiving Station, Dundee University, Scotland.

ments of O_3 were made in Garmisch-Partenkirchen, ~40 km south of Hohenpeissenberg, for 26 hours (Plate 2). Plate 2 impressively shows how the thin tongue of ozone-rich air (concentrations ranging from 65 to 110 ppb), caused by the intrusion, descended from ~6 km to 3 km asl within 26 hours. It was sandwiched between air masses containing only 40–60 ppb of O_3. This is especially obvious after May 29, 0400 UTC, when a 4000-m-thick layer of uniformly moderate O_3 concentrations lay above the O_3 tongue.

Plate 3 shows the time-height section of the stratospheric O_3 tracer concentrations as obtained with the FLEXPART particle model for the grid column containing Hohenpeissenberg and Garmisch-Partenkirchen. On May 27 the tropopause in the model was at around 12 km. One day later, just at the time of the ozone sounding (marked by R in Plate 3), the intrusion appeared at the lidar site above 4 km. This layer corresponds rather well to the O_3 peak in the sounding data (compare Figure 6). In possible contrast to the ozone-sounding data, however, this peak seems to be connected directly to the stratosphere (though O_3 tracer concentrations were very low between 7 and 8 km). The calculated O_3 tracer concentrations were somewhat lower than the observed O_3 concentrations, but the missing O_3 could probably be explained by mixture with tropospheric O_3, which is not accounted for in the simulation.

Shortly after the ozone sounding at Hohenpeissenberg, the core of the simulated intrusion was located directly in the grid column, and hence O_3 tracer concentrations were very high (>200 ppb) between 6 and 9 km. These concentrations are probably too high to be realistic. Unfortunately, there were no observations made to which the model results could be compared at this time, but lidar measurements have shown peak concentrations in the upper troposphere of the order of 200 ppb on one occasion in 1996.

The lidar measurements started just after the modeled tracer concentrations had decreased to lower values. The stratospheric filament known from the lidar data (compare Plate 2) is also evident in the model results, although it is much thicker than in the measurement data. This is not surprising, since the resolution of the ECMWF model is much coarser than that of the lidar data. However, in correspondence to the

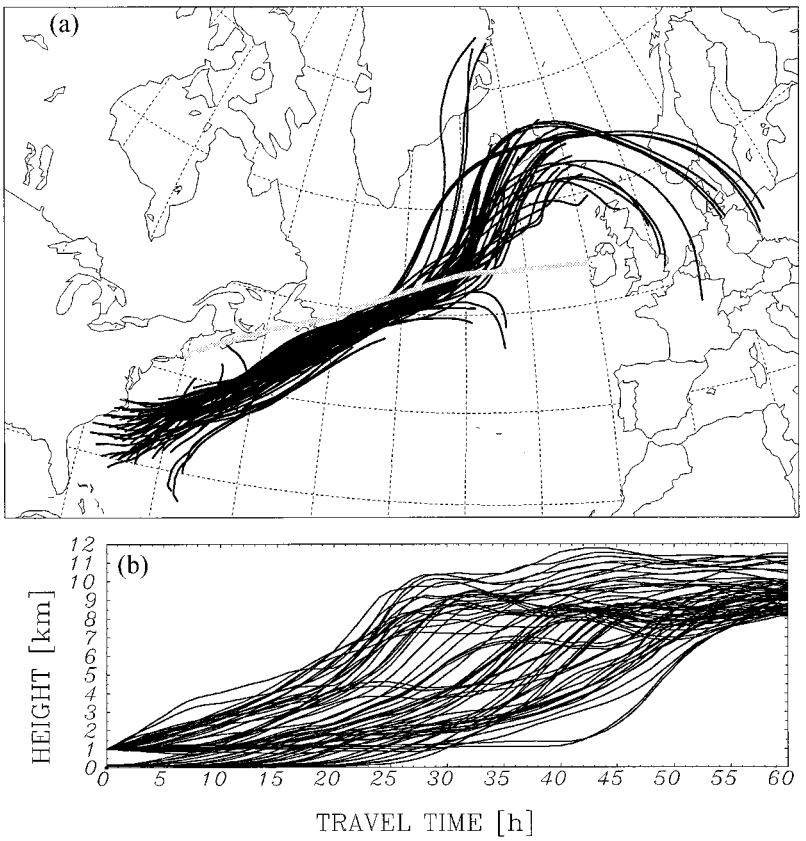

Figure 5. Coherent ensemble of trajectories ascending by at least 8000 m started on May 26, 1997, at 1800 UTC. (a) A horizontal projection of the CET; (b) a time-height profile of the trajectories. The thick light shaded line marks the flight leg of the MOZAIC aircraft between 70°W and 10°W.

measurements, the filament descended from initially 6 km to ~3 km. Very low concentrations (<1 ppb) were also modeled at the surface.

The structure of high measured O_3 concentrations found between 6 and 8 km on May 29 at 0000 UTC corresponded to very low modeled stratospheric O_3 tracer concentrations. As will be shown later in this section, this layer was characterized by very low PV values, and the trajectories arriving in this layer ascended. The FLEXPART model results suggest that only a minor fraction of stratospheric air may have been present in this air mass. The other prominent tropospheric structure in the lidar data, at 8 km on May 29 between 0700 and 1200 UTC, was completely missing in the FLEXPART results with the stratospheric tracer. Also of interest is the second intrusion that occurred on May 30. According to the model results, both intrusions were clearly separated from each other but nevertheless occurred within the same synoptic system, which remained almost stationary during that time period.

At the Zugspitze summit (2962 m), just about 10 km to the southwest of the lidar site, a moderate O_3 peak (64 ppb) was observed on May 29 at noon that was accompanied by a drop in relative humidity to 10%. This confirms that the stratospheric intrusion reached the mountain top.

A clear signature of the stratospheric intrusion was recorded at the higher (3580 m) Jungfraujoch observatory, where the intrusion also penetrated deeper into the troposphere (compare Plate 1). The ^{7}Be concentrations measured between May 27 and 31 were among the highest so far on the 2-year record (from April 1996 to July 1998) at Jungfraujoch, emphasizing the stratospheric nature of this air mass. The O_3 mixing ratio increased to 89 ppb, while the relative humidity dropped to 7% in the evening on May 28 (Figure 7). A second O_3 peak and a drop in relative humidity on May 29 were obviously also caused by the intrusion. The short-term fluctuations of O_3 and relative humidity are typical during stratospheric intrusions at mountain peaks. During daytime they are likely to be caused by local contamination with boundary layer air brought up from the valleys by upslope flows. The O_3 peak at Jungfraujoch in the evening on May 30 (Figure 7) was due to the second intrusion mentioned above. This air mass also arrived at Mount Cimone (10.42°E, 44.12°N, 2165 m), the highest peak in the northern Apennines, where O_3 concentrations of 97 ppb were measured on May 30 and 31.

To elucidate the origin of the different air masses seen in the lidar profile, 178-hour backward trajectories were initialized every 250 m asl along the lidar axis from 1250 to 8250 m asl. It should be kept in mind that the accuracy of the trajectories decreases with time, and after 72 to 96 hours their position (both horizontally as well as vertically) may be significantly in error [*Stohl*, 1998], typical errors being 15–20% of the transport distance. Plate 4 shows the trajectories arriving at the lidar measurement site on May 28 at 2200 UTC. Trajectories ending at the lidar site close to the ground (below 2250 m) ascended from the North Atlantic boundary layer, thus explaining the low O_3 concentrations within that layer. Most of the trajectories ending between 2500 and 3750 m (i.e., a layer of interme-

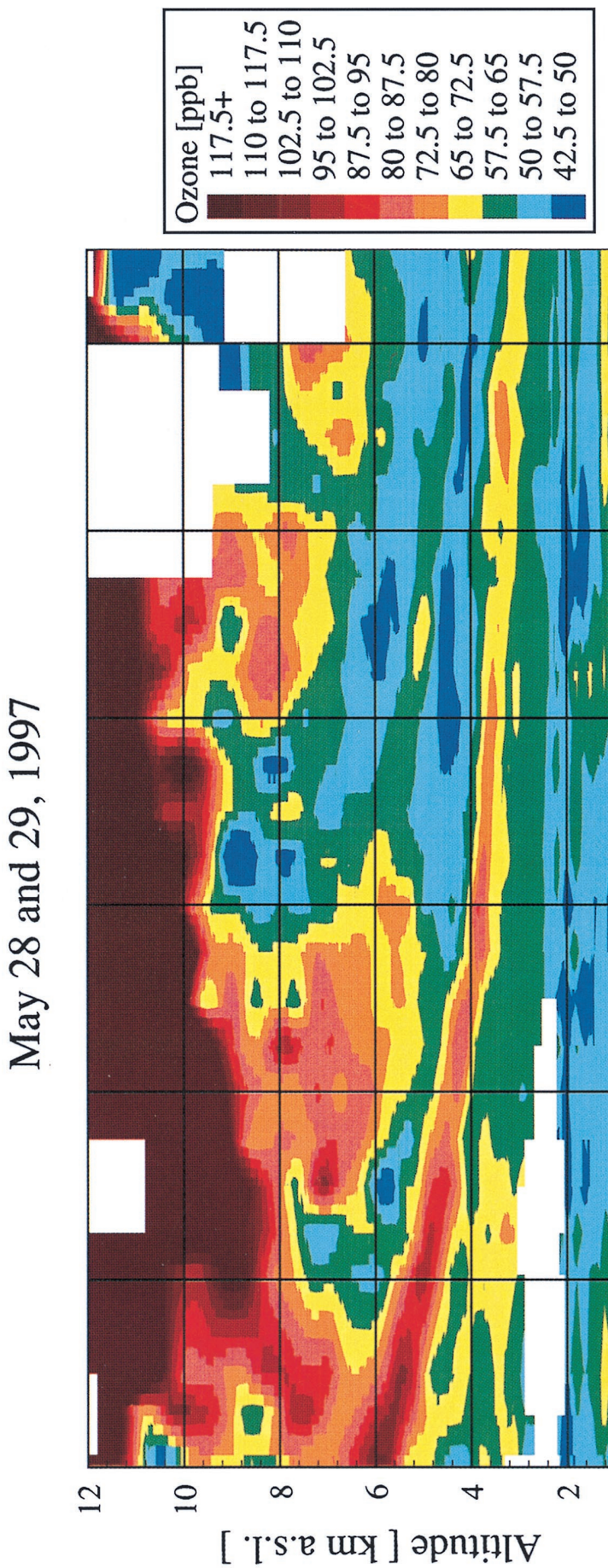

Plate 2. Time-height section of ozone as captured by lidar measurements in Garmisch-Partenkirchen. Time is in central European time (CET), which is 1 hour ahead of UTC. The white areas correspond to cloud layers, for which no useful data have been obtained.

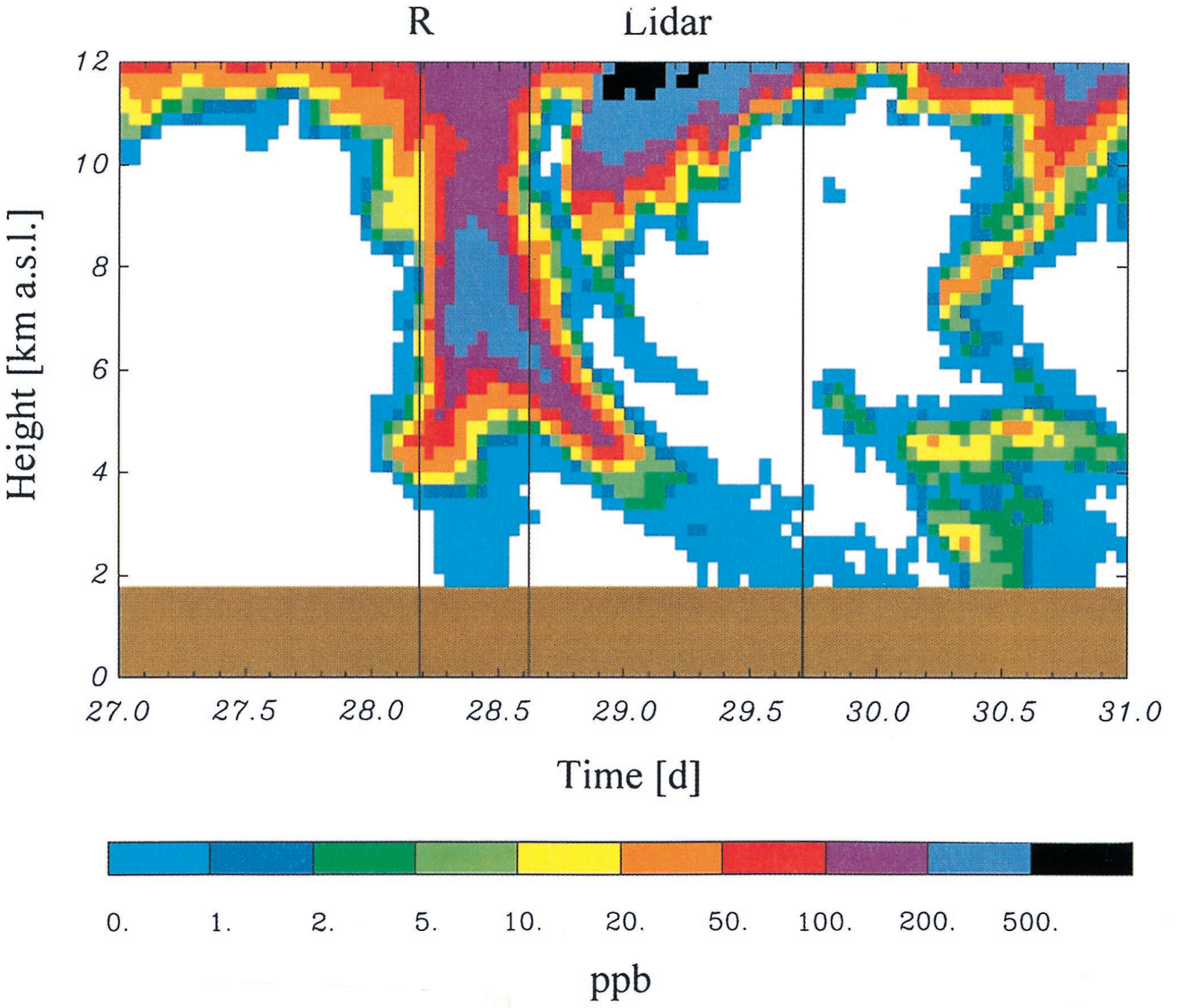

Plate 3. Time-height section of the stratospheric ozone tracer concentrations calculated with FLEXPART for the grid column corresponding to the Hohenpeissenberg ozone sonde and the lidar measurement sites. The brown shading gives the altitude of the model topography, the thick vertical line marked with R shows the time of the ozone sounding, and the two thin vertical lines indicate the start and the end of the lidar measurements.

diate O_3 concentrations) showed little vertical motion or weak descent and had low PV values, whereas the trajectories ending between 4000 m and 4750 m (i.e., within the filament of high O_3 concentrations) descended strongly and had their origin at northerly latitudes. Between 4000 and 4750 m, PV was also increased (~0.8 pvu) compared to the layers below and above (Plate 4, bottom). Along the back trajectories, PV values exceeded 1.6 pvu, and maximum values were close to 4 pvu, showing that this air came from the lower stratosphere. Trajectories terminating at 5000 m and above showed a short phase of descent prior to their arrival, but before that, they ascended from the middle troposphere. PV along the 5000-m trajectory never exceeded 1 pvu. It is thus obvious that the low O_3 concentrations immediately above the stratospheric filament were of tropospheric origin.

Also of interest were the high O_3 concentrations between 6 and 8 km, close to the tropopause (Plate 2). Because of the peak mixing ratios near 100 ppb and the descending behavior, *Eisele et al.* [1999] speculated that such secondary structures above and behind a stratospheric intrusion, which are quite often seen in lidar data, may indicate additional O_3 transfer from the stratosphere to the troposphere. The PV, however, was very low in this layer (the minimum PV was 0.1 pvu) and humidity measurements of the radio sondes in Munich (90 km northnortheast of the lidar site) and Innsbruck (40 km to the southeast) on May 28 at 2300 UTC and May 29 at 0000 UTC showed the presence of moist air in this layer. The relative humidity calculated with respect to the saturation pressure over liquid water exceeded 40%. In addition, the trajectories demonstrate that this air was of tropospheric origin, since they came from middle latitudes and the PV along them never exceeded 0.4 pvu (Plate 4).

On May 29 at 0900 UTC (Plate 5), the lowermost layer of the Atlantic boundary layer air had shrunk to 1500–1750 m. Above that layer the trajectories descended, but only those terminating at 2750 and 3000 m descended strongly and only

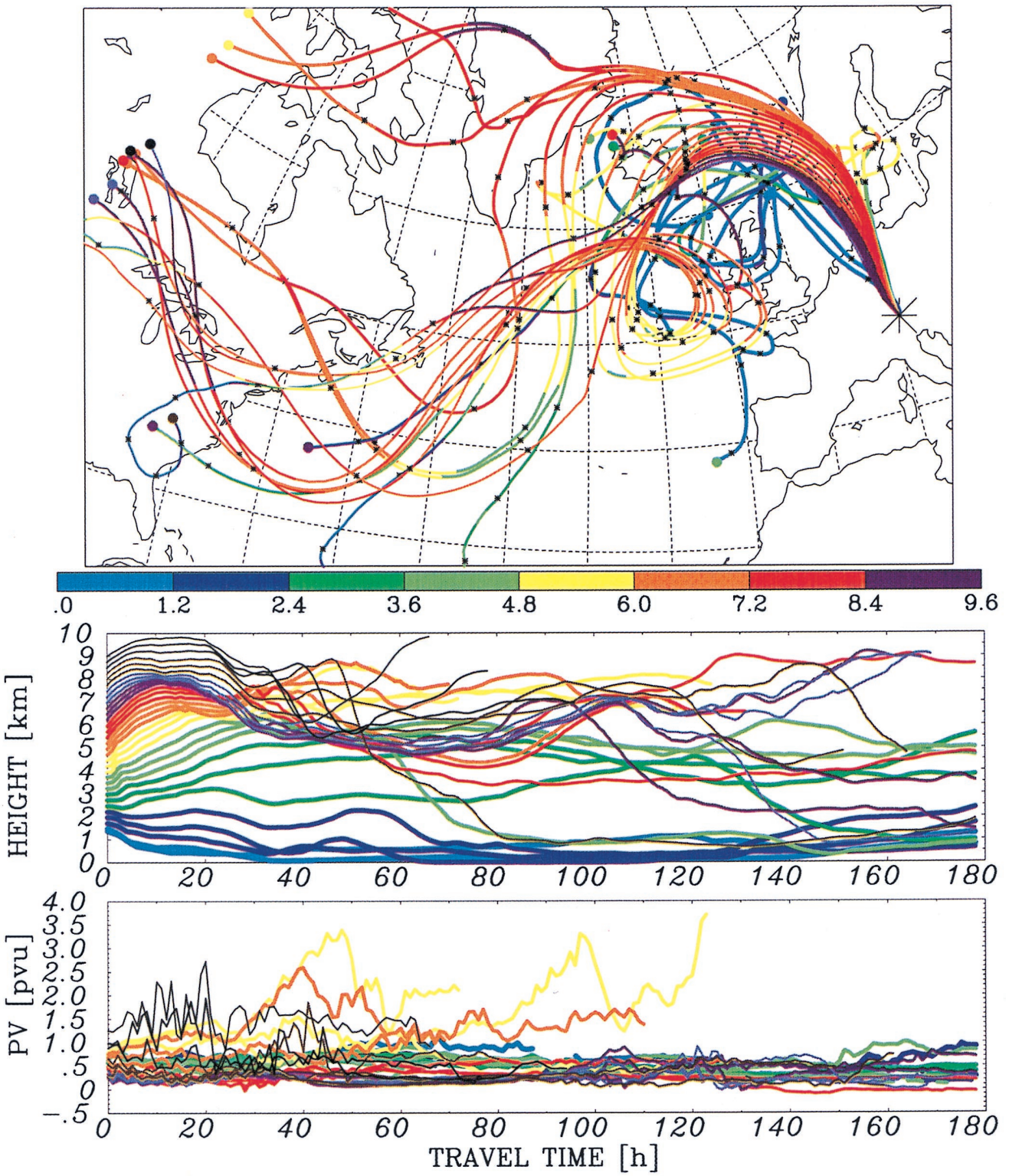

Plate 4. The 178-hour three-dimensional backward trajectories terminating at the lidar measurement site every 250 m in height on May 28 at 2200 UTC (corresponding to 23 hours in Plate 2): (top) a horizontal projection of the trajectories, with the color-coding according to the label bar referring to the actual heights (in km asl). Positions are marked with asterisks every 24 hours. The dots at the trajectory starting points indicate the heights where the trajectories terminated along the lidar profile, with the color code of the dots corresponding to Plate 4 (middle). The same information is also provided by the line widths (thinner lines representing trajectories terminating at higher levels). (middle) Time-height profiles of the trajectories with both color and line width indicating their ending height at $T = 0$. (bottom) PV along the different trajectories with both the line color and line width corresponding to Plate 4 (middle). PV data are sometimes missing in the boundary layer in unstable situations. Some of the trajectories were terminated because they exited the computational domain. Note that time is backward along the trajectories.

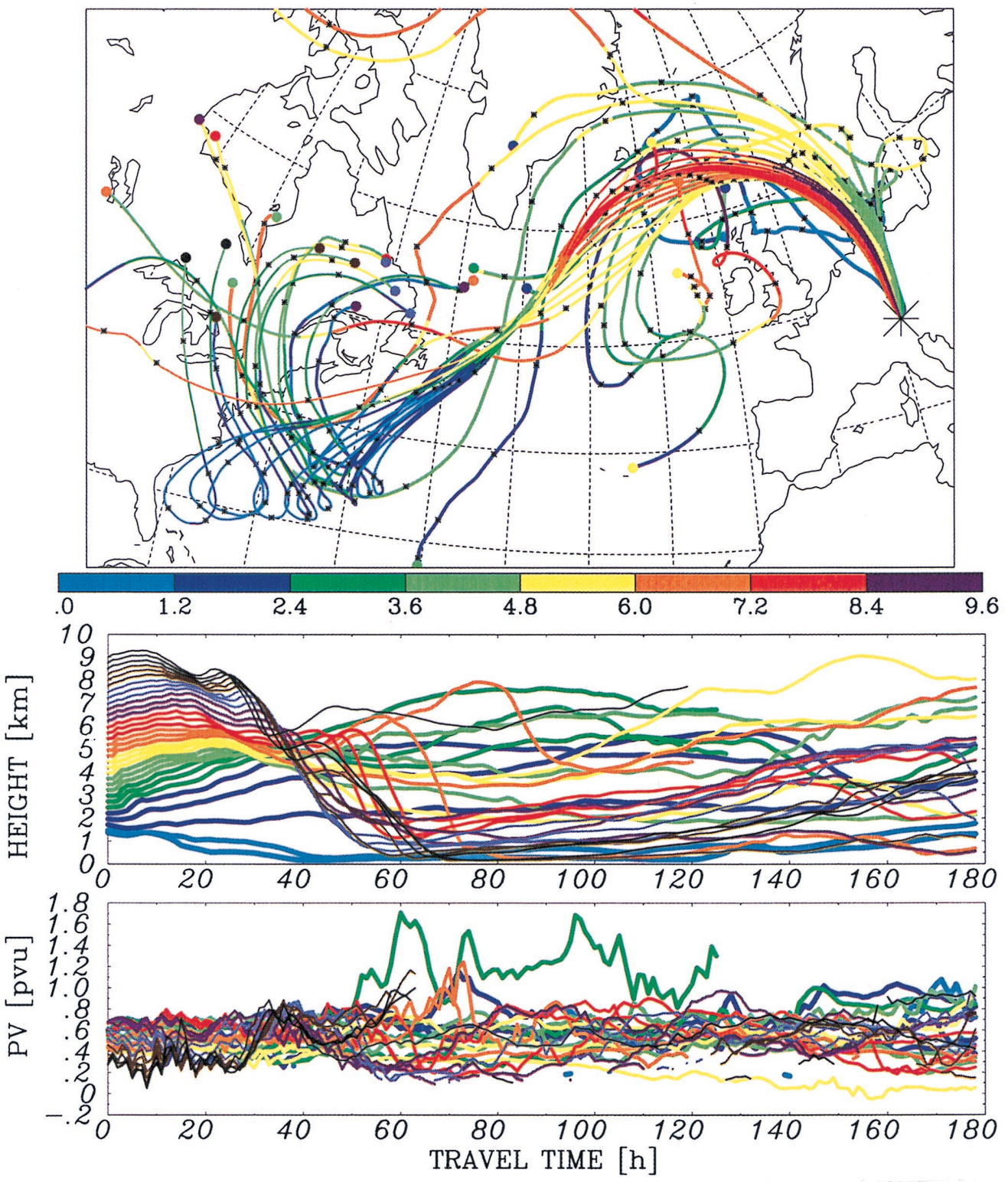

Plate 5. Same as Plate 4, but for trajectories terminating on May 29 at 0900 UTC (corresponding to 34 hours in Plate 2).

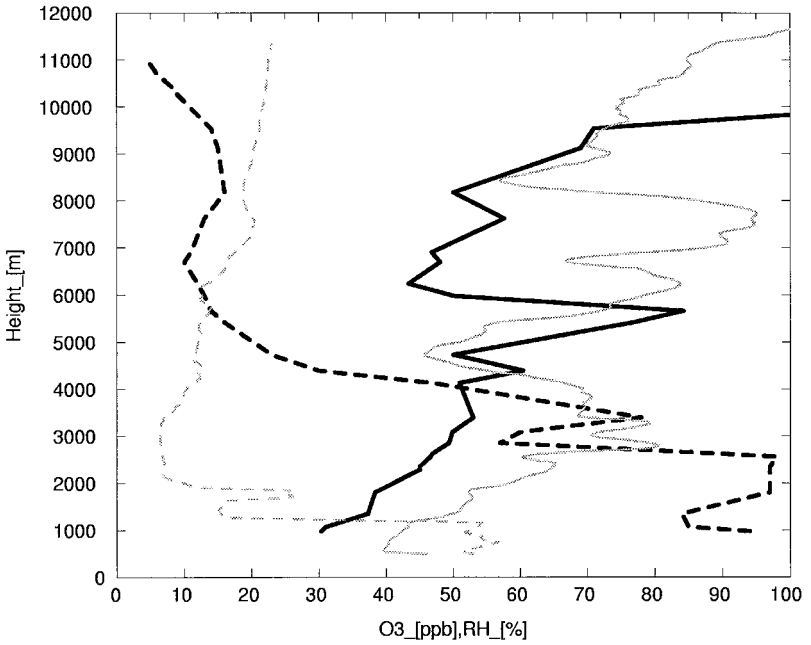

Figure 6. Vertical profiles of relative humidity (dashed lines) and ozone (solid lines) at the radiosounding stations Hohenpeissenberg on May 28, 1997, at 0500 UTC (thick solid lines) and Payerne on May 28, 1997, at 1100 UTC (thin shaded lines).

the 2750-m trajectory reached PV levels of >1.6 pvu, indicating a stratospheric origin. Trajectories terminating above the thin stratospheric tongue ascended and showed very low PV values.

The structure with high O_3 concentrations (>80 ppb) located at 8000 m between 0700 and 1200 UTC on May 29 had PV values of some 0.3 pvu. PV along the trajectories ending in this layer fluctuated strongly but never exceeded 1 pvu. The relative humidity obtained from the radiosonde started in Munich on May 29 at 1200 UTC peaked at 61% at 8000 m (Figure 8). Since the saturation water vapor pressure over ice is lower than over liquid water, the air was almost saturated with respect to ice, a clear indication that there was no stratospheric contribution to the high O_3 concentrations. The trajectories strongly suggest that this air came from the North American boundary layer. Although their accuracy at the starting point (178 hours back in time) is probably rather low, they already got close to the American coast <72 hours back in time, when their general pathway should be still reliable. In addition, owing to the coherency of the transport, the accuracy should be higher than usual [*Cohen and Kreitzberg*, 1997]. During its passage over the Atlantic Ocean the air became entrained in

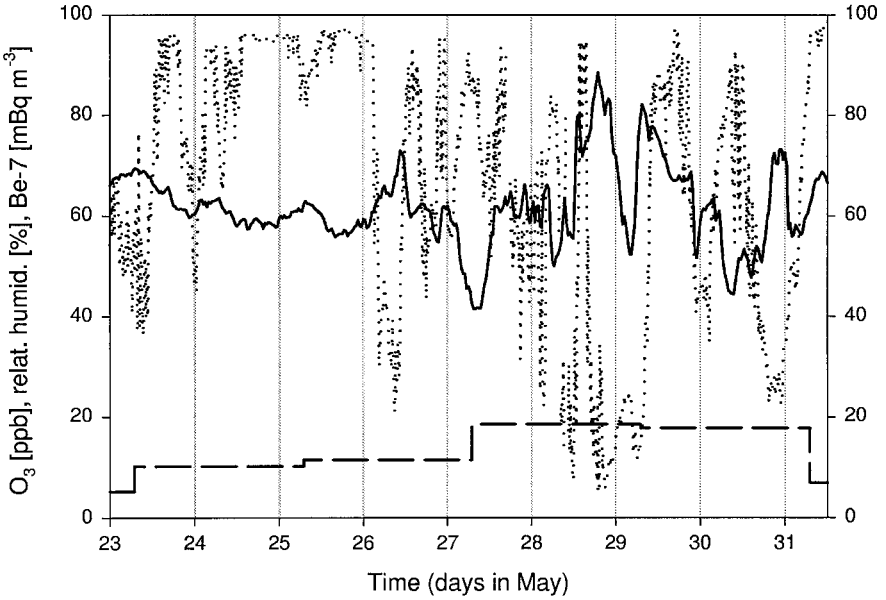

Figure 7. Concentrations of ozone (solid line) and ^{7}Be (dashed line), and relative humidity (dotted line) at Jungfraujoch during May 23 to 31, 1997; the ^{7}Be samples have a resolution of 48 hours.

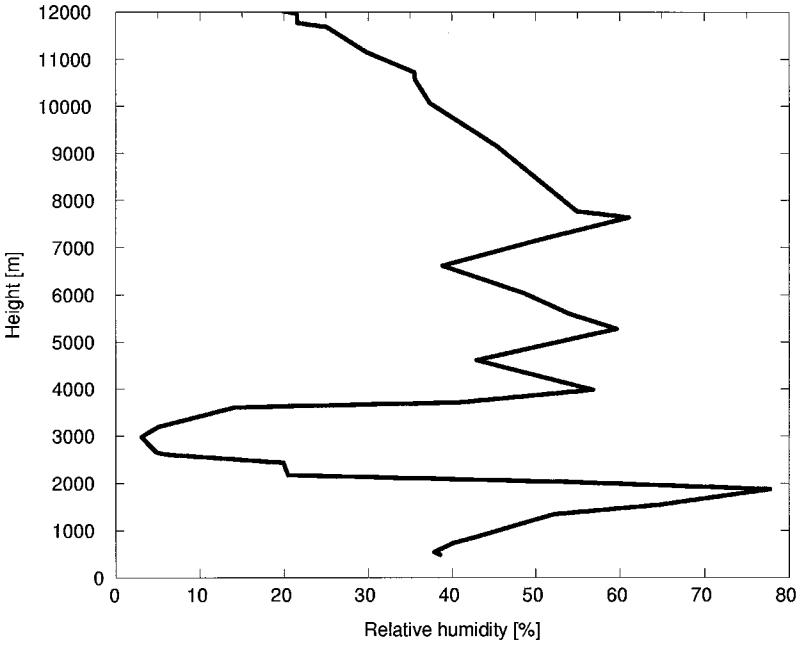

Figure 8. Vertical profile of relative humidity obtained from the radiosonde started in Munich on May 29 at 1200 UTC.

the WCB (Figure 5) and was lifted to the jet stream level within ~24 hours.

To confirm further the North American origin of the low-PV O_3 structure, we made a simulation with FLEXPART, releasing particles continuously at the surface in North America. Material of this North America tracer first appeared over Europe on May 26, but its concentrations at the lidar site (Figure 9) were very low at this time. The North America tracer was advected at much higher concentrations at the backside of and above the intruding stratospheric air. It can also be seen that

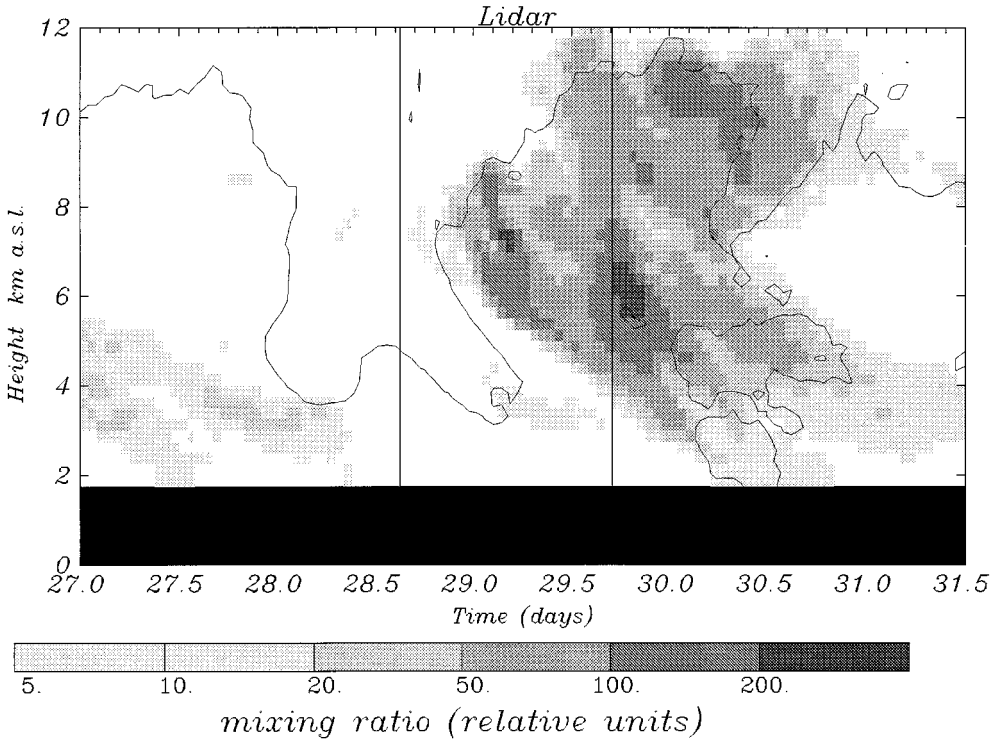

Figure 9. Time-height section of the North America tracer mixing ratios in relative units calculated with FLEXPART for the grid column corresponding to the lidar measurement site; the solid area gives the altitude of the model topography, the two vertical lines indicate the start and the end of the lidar measurements. Also shown is the 2-ppb contour line of the stratospheric ozone tracer (repeated from Plate 3).

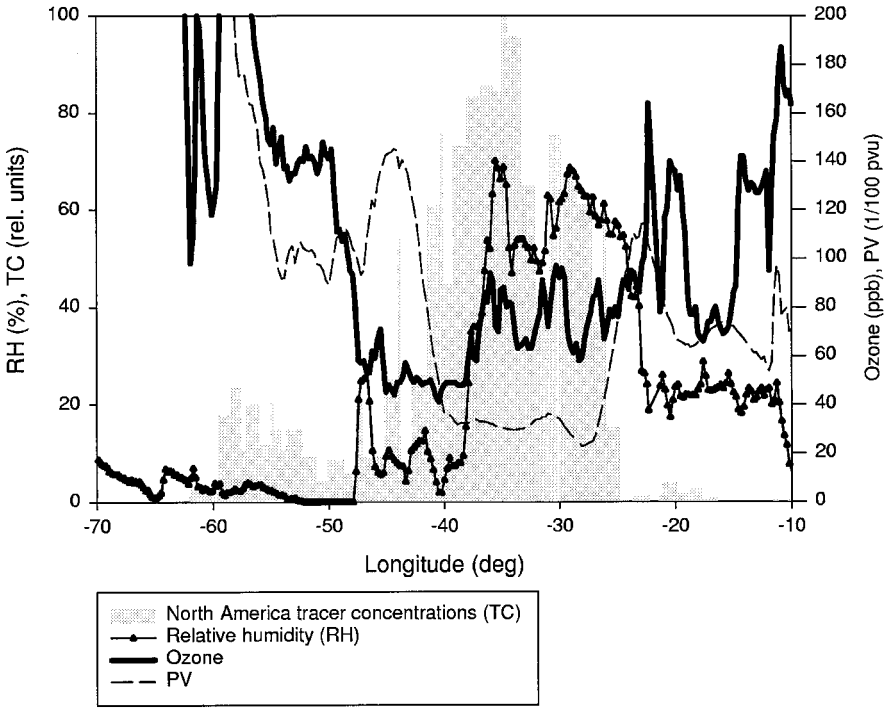

Figure 10. Ozone, relative humidity, PV, and North America tracer concentrations along the MOZAIC aircraft flight leg shown in Figure 5.

there is a small vertical gap <1 km wide above the stratospheric filament, where neither the stratospheric O_3 tracer nor the North America tracer was present. This could probably be identified with the thin layer of very low measured O_3 concentrations that was located just above the stratospheric filament (compare Plate 2). Trajectory calculations showed that this air came from the (upper) free troposphere over North America. Above that layer the concentrations of the North America tracer are relatively high, and the measurements show pockets of high O_3 concentrations.

According to the above results we propose that the high-O_3 pockets were produced photochemically in the continental plume of North America. The meteorological conditions at the time when the back trajectories terminating along the lidar axis resided over North America were very conducive to photochemical O_3 formation. On May 24, high O_3 concentrations were measured at several locations along the American east coast. Concentrations at a background site in Virginia (77.32°W, 37.64°N, 100 m asl), which is in the center of our back trajectory bundle, reached 95 ppb (D. Parrish, personal communication, 1998).

It is also of interest that the model results suggest that on May 30 the North America tracer has been mixed into air that descended from the stratosphere within the second stratospheric intrusion (Figure 9). This was caused by the fact that the North America tracer was lifted up to the tropopause within the WCB, before it descended with the dry intrusion. It is known that the airstream related to a dry intrusion is composed of both upper tropospheric as well as stratospheric air [*Browning*, 1990]. Thus, for this case it is virtually impossible to separate between O_3 of stratospheric and of North American origin. Both may have contributed to the O_3 increases seen at Zugspitze and Jungfraujoch on May 30 (see Figure 7). Since the tropospheric air also descended from high levels, relative humidity was, again, very low during the O_3 peak.

Further evidence for the correctness of the scenario of a North American origin of the high O_3 pockets in the upper troposphere as indicated above comes from three MOZAIC flights that crossed the WCB in the middle of the Atlantic Ocean on May 28. During all three passages of the WCB the measured O_3 concentrations showed peaks of around 100 ppb, while relative humidity was high and potential vorticity interpolated to the aircraft positions was very low (for one flight even below zero). Since all three flights showed similar characteristics, we present data from only one flight in more detail, which departed from Atlanta on May 27 at 2100 UTC and arrived at Frankfurt on May 28 at 0500 UTC. We focus on the part of the flight between 70°W and 10°W (shown in Figure 5) and show the variation of O_3, relative humidity, PV, and North America tracer concentrations (Figure 10) along this leg. During this period (2236 UTC on May 27 to 0314 UTC on May 28) the airliner flew constantly at 10,680 m asl.

Starting at 70°W, both PV and O_3 were very high (9 pvu and 490 ppb), while relative humidity was close to zero and no North America tracer was present. Clearly, the airliner flew in the stratosphere. At 60°W, both O_3 and PV started to fluctuate, and low concentrations of the North America tracer were present. Relative humidity was still low, though. At 50°W, O_3 suddenly dropped to 40–50 ppb, while PV stayed at upper tropospheric levels (0.8–1.4 pvu). Relative humidity was slightly higher than before. However, at 38°W, relative humidity rose to 70%, while PV dropped to 0.3 pvu, characteristic for the tops of moist airstreams ascending from the boundary layer [*Wernli and Davies*, 1997]. The North America tracer showed two peaks which corresponded to the peaks in relative humidity, evidencing that the air contained within the WCB was of

North American origin. This was confirmed by the calculation of back trajectories ending at the aircraft positions, which reached the North American boundary layer somewhat to the west of the source area of the WCB depicted in Figure 5. O_3 concentrations within the WCB were positively correlated with relative humidity, in contrast to the stratospheric part of the flight. Specifically, two O_3 peaks of 94 and 97 ppb, respectively, corresponded well with humidity peaks. These O_3 concentrations are of the same level as the highest concentrations seen later in the Payerne ozone sounding (Figure 6) and in the lidar data (Plate 2). This, together with the particle model calculations, the trajectory calculations (Figure 5 and Plate 5), the satellite image (Figure 4), and the fact that an ozone episode occurred at the North American east coast at the time when the long-range transport started, suggests a common North American source of the O_3. When the aircraft left the WCB at ~25°W, humidity dropped, while O_3 and PV increased. Obviously, for the remainder of the leg, the aircraft flew in the tropopause region, with partly stratospheric characteristics.

5. Conclusions

In this paper an episode of enhanced O_3 concentrations in the free troposphere over Europe was analyzed in detail. Measurement data showed stratospheric air penetrating deep into the lower troposphere, reaching ~700 hPa in the Alpine region. Trajectory calculations suggested that the intrusion penetrated even deeper, probably to the 900 hPa level, over Greece and western France. By combining measurement data with model results it was possible to understand the large-scale transport processes related to this intrusion and, specifically, to distinguish structures of tropospheric and of stratospheric origin. Two days after the intrusion discussed in this paper a separate second one occurred, while the large-scale weather pattern at 500 hPa remained virtually unchanged. Both intrusions left clear signatures in the measurements of stratospheric tracers at mountain observatories. The fact that two clearly separated stratospheric intrusions may occur within the same synoptic system has important implications for calculating the total air mass (or O_3) transfer from the stratosphere to the troposphere. Measurements at mountain summits indicate that such multiple events may occur several times per year. We do not report an O_3 flux across the tropopause for this episode, since we found its value to be highly sensitive to the size of the calculation domain and the time period considered, which makes any such number almost meaningless.

Behind and above the stratospheric intrusion studied in this paper, air with a lower tropospheric origin was advected. The model calculations revealed that some parcels with particularly high O_3 mixing ratios (up to 100 ppb) originated in the North American boundary layer during a period conducive to photochemical O_3 formation; got entrained into a WCB above the North Atlantic, where they were transported in a very organized manner; and finally arrived with the outflow of the WCB in the upper troposphere over Europe. Although trajectory calculations are rather uncertain for such long travel distances, the good overall agreement between the model calculations and the measurements during the period studied leads us to propose that the O_3 was produced in the continental plume of North America. O_3 and humidity observations by a MOZAIC airliner that passed the WCB over the middle of the Atlantic Ocean confirmed our proposed scenario. The identification of the nature of this air mass was greatly favored by the coherency of the transport: first, because trajectory errors in coherent flows are much lower than usual [*Cohen and Kreitzberg*, 1997]; and second, because it prevented mixing with surrounding air masses, conserving high O_3 concentrations within relatively large volumes which were resolvable by the lidar and attracted our attention. This is in contrast to other transport episodes, where air parcels are drawn asunder because of chaotic advection [*Ottino*, 1989; *Pudykiewicz and Koziol*, 1998].

Transport of polluted air masses from North America to the Azores has been discussed previously by *Parrish et al*. [1998], but their maximum O_3 concentrations (~70 ppb) were clearly below those found in our data. However, in our case the air was advected northward, where radiation is weaker than at more southerly latitudes, and it was lifted to upper tropospheric levels, where water vapor concentrations are lower than in the maritime boundary layer and transport speeds are much higher. All these factors strongly favor the occurrence of destruction-free long-range transport of O_3. This may be the first time that O_3 imported from North America has been identified with some confidence over Europe.

Eisele et al. [1999] report on a similar episode in 1996 which lasted for a total of 5 days (May 28 to June 1). Preliminary trajectory results indicate that some of the descending O_3 maxima also observed between 4 and 11 km asl in this case may, again, be related to intercontinental transport. Recently, *Arnold et al*. [1997] reported a case where aircraft measurements showed high concentrations of sulfur dioxide and condensation nuclei at 9000 m asl north of Ireland, which they related to the presence of polluted boundary layer air from North America. Although *Arnold et al*. [1997] did not refer to a WCB as being responsible for the uplifting, an inspection of weather maps suggests that this was very probably the case. This indicates that the findings described in this paper are not unique. In addition, *Wernli and Davies* [1997] found that the area comprising the Gulf of Mexico, the Caribbean, and the eastern seaboard of North America is the most preferred entrance region for WCBs in the Northern Hemisphere. Since WCBs, associated with fronts, are frequent phenomena in the extratropical atmosphere, intercontinental O_3 transport as described in this paper may indeed occur quite often. Thus transport of O_3 from North America to Europe may be more important than previously thought. It is probably the lack of suitable measurement data in the upper troposphere that hitherto made the identification of such episodes improbable.

WCBs may be important not only for the long-range transport of O_3 but, in a broader sense, also for the export of pollution from the atmospheric boundary layer into the free troposphere. Of course, soluble chemical species and aerosols will be quickly washed out by the strong precipitation beneath the WCB cloud band. However, for nonsoluble species the role of WCBs for the transport of pollutants into the (upper) free troposphere may have been underestimated in the past. Even soluble species like sulfur dioxide may not be washed out completely as suggested by the study of *Arnold et al*. [1997] and may contribute to aerosol formation in the tropopause region. More research is clearly needed along these lines.

Acknowledgments. This study was part of the EU research project "Vertical Ozone Transports in the Alps" (VOTALP), funded by the European Commission under Framework Programme IV, Environment and Climate, contract ENV4-CT95-0025, and by the governments of Switzerland and Austria. The authors are grateful to all colleagues involved in the measurements or in the processing of data

for the project and to the whole VOTALP community for stimulating discussions. S. Hübener from the University of Berne provided ^{7}Be measurements from Jungfraujoch, and H. E. Scheel made the measurement data from Zugspitze available. ECMWF and Deutscher Wetterdienst admitted access to ECMWF data within the special project "Validation of trajectory calculations." Ozone sounding data from Hohenpeissenberg were made available by W. Fricke and H. Claude from Deutscher Wetterdienst, the Swiss Meteorological Institute provided meteorological data from Jungfraujoch and ozone sounding data from Payerne, and the Bundesamt für Umwelt, Wald und Landwirtschaft (Switzerland) supplied us with ozone data from Jungfraujoch. P. Bonasoni and D. Parrish provided ozone data from Mount Cimone and from the North American east coast, respectively. Our warmest thanks go to A. Marenco and G. Athier, who made the MOZAIC data available for this study. TOVS data were prepared by NCEP and downloaded from http://auc.dfd.dlr.de/info/AUC/index.html, and Meteosat water vapor images were provided by the Central Institute of Meteorology and Geodynamics, Vienna. Special thanks are due to H. Wernli and two anonymous referees for their detailed reviews of an earlier version of this paper. The comments of P. Fabian and G. Wotawa and the generous support by W. Seiler are appreciated.

References

Appenzeller, C., and H. C. Davies, Structure of stratospheric intrusions into the troposphere, *Nature*, *358*, 570–572, 1992.

Arnold, F., J. Schneider, K. Gollinger, H. Schlager, P. Schulte, D. E. Hagen, P. D. Whitefield, and P. van Velthoven, Observation of upper tropospheric sulfur dioxide- and acetone-pollution: Potential implications for hydroxyl radical and aerosol formation, *Geophys. Res. Lett*., *24*, 57–60, 1997.

Austin, J. F., and R. P. Midgley, The climatology of the jet stream and stratospheric intrusions of ozone over Japan, *Atmos. Environ*., *28*, 39–52, 1994.

Baumann, K., and A. Stohl, Validation of a long-range trajectory model using gas balloon tracks from the Gordon Bennett Cup 95, *J. Appl. Meteorol*., *36*, 711–720, 1997.

Beekmann, M., et al., Regional and global tropopause fold occurrence and related ozone flux across the tropopause, *J. Atmos. Chem*., *28*, 29–44, 1997.

Bethan, S., G. Vaughan, C. Gerbig, A. Volz-Thomas, H. Richer, and D. A. Tiddeman, Chemical air mass differences near fronts, *J. Geophys. Res*., *103*, 13,413–13,434, 1998.

Browning, K. A., Organization of clouds and precipitation in extratropical cyclones, in *Extratropical Cyclones: The Erik H. Palmen Memorial Volume*, edited by C. Newton and E. Holopainen, pp. 129–153, Am. Meteorol. Soc., Boston, Mass., 1990.

Browning, K. A., The dry intrusion perspective of extra-tropical cyclone development, *Meteorol. Appl*., *4*, 317–324, 1997.

Browning, K. A., Mesoscale aspects of extratropical cyclones: An observational perspective, in *The Life Cycles of Extratropical Cyclones*, edited by M. A. Shapiro and S. Grønås, pp. 265–283, Am. Meteorol. Soc., Boston, Mass., 1999.

Browning, K. A., and N. M. Roberts, Structure of a frontal cyclone, *Q. J. R. Meteorol. Soc*., *120*, 1535–1557, 1994.

Browning, K. A., and N. M. Roberts, Variation of frontal and precipitation structure along a cold front, *Q. J. R. Meteorol. Soc*., *122*, 1845–1872, 1996.

Carlson, T. N., Airflow through midlatitude cyclones and the comma cloud pattern, *Mon. Weather Rev*., *108*, 1498–1509, 1980.

Cohen, R. A., and C. W. Kreitzberg, Airstream boundaries in numerical weather simulations, *Mon. Weather Rev*., *125*, 168–183, 1997.

Danielsen, E. F., Stratospheric-tropospheric exchange based on radioactivity, ozone and potential vorticity, *J. Atmos. Sci*., *25*, 502–518, 1968.

Davies, T. D., and E. Schuepbach, Episodes of high ozone concentrations at the surface resulting from transport down from the upper troposphere/lower stratosphere: A review and case studies, *Atmos. Environ*., *28*, 53–68, 1994.

Derwent, R. G., P. G. Simmonds, S. Seuring, and C. Dimmer, Observation and interpretation of the seasonal cycles in the surface concentrations of ozone and carbon monoxide at Mace Head, Ireland from 1990 to 1994, *Atmos. Environ.*, *32*, 145–157, 1998.

Eisele, H., H. E. Scheel, R. Sladkovic, and T. Trickl, High-resolution lidar measurements of stratosphere-troposphere exchange, *J. Atmos. Sci*., *56*, 319–330, 1999.

European Centre for Medium-Range Weather Forecasts (ECMWF), User guide to ECMWF products 2.1, *Meteorol. Bull. M3.2*, Reading, England, U.K., 1995.

Helten, M., H. G. Smit, W. Sträter, D. Kley, P. Nedelec, M. Zöger, and R. Busen, Calibration and performance of automatic compact instrumentation for the measurement of relative humidity from passenger aircraft, *J. Geophys. Res*., *103*, 25,643–25,652, 1998.

Holton, J. R., P. H. Haynes, E. M. McIntyre, A. R. Douglass, R. B. Rood, and L. Pfister, Stratosphere-troposphere exchange, *Rev. Geophys*., *33*, 403–439, 1995.

Jennings, S. G., T. G. Spain, B. G. Doddridge, H. Maring, B. P. Kelly, and A. D. A. Hansen, Concurrent measurements of black carbon aerosol and carbon monoxide at Mace Head, *J. Geophys. Res*., *101*, 19,447–19,454, 1996.

Koch, D. M., and M. E. Mann, Spatial and temporal variability of ^{7}Be surface concentrations, *Tellus*, *Ser. B*, *48*, 387–396, 1996.

Kowol-Santen, J., Numerische Analysen von Transport- und Austauschprozessen in der Tropopausenregion der mittleren Breiten, *Mitt. Inst. Geophys. Meteorol. Univ. Köln*, *123*, 186 pp., 1998.

Lamarque, J.-F., A. O. Langford, and M. H. Proffitt, Cross-tropopause mixing of ozone through gravity wave breaking: Observation and modeling, *J. Geophys. Res*., *101*, 22,969–22,976, 1996.

Liu, S. C., M. Trainer, F. C. Fehsenfeld, D. D. Parrish, E. J. Williams, D. W. Fahey, G. Hubler, and P. C. Murphy, Ozone production in the rural troposphere and the implications for regional and global ozone distributions, *J. Geophys. Res*., *92*, 4191–4207, 1987.

Marenco, A., et al., Measurement of ozone and water vapor by airbus in-service aircraft: The MOZAIC airborne program, An overview, *J. Geophys. Res*., *103*, 25,631–25,642, 1998.

Ottino, J. M., *The Kinematics of Mixing: Stretching, Chaos, and Transport*, 364 pp., Cambridge Univ. Press, New York, 1989.

Parrish, D. D., J. S. Holloway, M. Trainer, P. C. Murphy, G. L. Forbes, and F. C. Fehsenfeld, Export of North American ozone pollution to the North Atlantic Ocean, *Science*, *259*, 1436–1439, 1993.

Parrish, D. D., M. Trainer, J. S. Holloway, J. E. Yee, M. S. Warshawsky, F. C. Fehsenfeld, G. L. Forbes, and J. L. Moody, Relationships between ozone and carbon monoxide at surface sites in the North Atlantic region, *J. Geophys. Res*., *103*, 13,357–13,376, 1998.

Poulida, O., R. R. Dickerson, and A. Heymsfield, Stratosphere-troposphere exchange in a midlatitude mesoscale convective complex, 1, Observations, *J. Geophys. Res*., *101*, 6823–6836, 1996.

Pudykiewicz, J. A., and A. Koziol, An application of the theory of kinematics of mixing to the study of tropospheric dispersion, *Atmos. Environ*., *24*, 4227–4244, 1998.

Roelofs, G.-J., and J. Lelieveld, Model study of the influence of cross-tropopause O_3 transports on tropospheric O_3 levels, *Tellus*, *Ser. B*, *49*, 38–55, 1997.

Ryall, D. B., R. H. Maryon, R. G. Derwent, and P. G. Simmonds, Modelling long-range transport of CFCs to Mace Head, Ireland, *Q. J. R. Meteorol. Soc*., *124*, 417–446, 1998.

Scheel, H. E., R. Sladkovic, and H.-J. Kanter, Ozone variations at the Zugspitze (2962 m a.s.l.) during 1996–1997, in *Proceedings of EUROTRAC-2 Symposium 1998*, vol. 1, edited by P. M. Borrell and P. Borrell, pp. 264–268, WIT Press, Southampton, England, 1999.

Steinbrecht, W., H. Claude, U. Köhler, and K. P. Hoinka, Correlation between tropopause height and total ozone: Implications for long-term changes, *J. Geophys. Res*., *103*, 19,183–19,192, 1998.

Stohl, A., Computation, accuracy and applications of trajectories—A review and bibliography, *Atmos. Environ*., *32*, 947–966, 1998.

Stohl, A., and N. E. Koffi, Evaluation of trajectories calculated from ECMWF data against constant volume balloon flights during ETEX, *Atmos. Environ*., *24*, 4151–4156, 1998.

Stohl, A., and P. Seibert, Accuracy of trajectories as determined from the conservation of meteorological tracers, *Q. J. R. Meteorol. Soc*., *125*, 1465–1484, 1998.

Stohl, A., and D. J. Thomson, A density correction for Lagrangian particle dispersion models, *Boundary Layer Meteorol*., *90*, 155–167, 1999.

Stohl, A., G. Wotawa, P. Seibert, and H. Kromp-Kolb, Interpolation errors in wind fields as a function of spatial and temporal resolution and their impact on different types of kinematic trajectories, *J. Appl. Meteorol*., *34*, 2149–2165, 1995.

Stohl, A., K. Baumann, G. Wotawa, M. Langer, B. Neininger, M. Piringer, and H. Formayer, Diagnostic downscaling of large scale

wind fields to compute local scale trajectories, *J. Appl. Meteorol*., *36*, 931–942, 1997.

Stohl, A., M. Hittenberger, and G. Wotawa, Validation of the Lagrangian particle dispersion model FLEXPART against large scale tracer experiment data, *Atmos. Environ*., *24*, 4245–4264, 1998.

Stohl, A., N. Spichtinger-Rakowsky, P. Bonasoni, H. Feldmann, M. Memmesheimer, H. E. Scheel, T. Trickl, S. Hübener, W. Ringer, and M. Mandl, The influence of stratospheric intrusions on alpine ozone concentrations, *Atmos. Environ*., in press, 1999.

Van Haver, P., D. de Muer, M. Beekmann, and C. Mancier, Climatology of tropopause folds at midlatitudes, *Geophys. Res. Lett*., *23*, 1033–1036, 1996.

Vaughan, G., Stratosphere-troposphere exchange of ozone, in *Tropospheric Ozone*, edited by I. S. A. Isaksen, pp. 125–135, D. Reidel, Norwell, Mass., 1988.

Wernli, H., A Lagrangian-based analysis of extratropical cyclones, II, A detailed case study, *Q. J. R. Meteorol. Soc*., *123*, 1677–1706, 1997.

Wernli, H., and H. C. Davies, A Lagrangian-based analysis of extratropical cyclones, I, The method and some applications, *Q. J. R. Meteorol. Soc*., *123*, 467–489, 1997.

Wirth, V., Diabatic heating in an axisymmetric cut-off cyclone and related stratosphere-troposphere exchange, *Q. J. R. Meteorol. Soc*., *121*, 127–147, 1995.

World Meteorological Organization (WMO), Atmospheric ozone 1985, *Rep. 20*, Global Ozone Res. and Monit. Proj., Geneva, Switzerland, 1986.

Zanis, P., E. Schuepbach, H. W. Gäggeler, and S. Hübener, Factors controlling beryllium-7 at Jungfraujoch in Switzerland, *Tellus*, *51*, 789–805, 1999.

A. Stohl, Lehrstuhl für Bioklimatologie und Immissionsforschung, Ludwig-Maximilians-Universität München, Am Hochanger 13, D-85354 Freising-Weihenstephan, Germany. (as@atmos1.met.forst.uni-muenchen.de)

T. Trickl, Fraunhofer-Institut für Atmosphärische Umweltforschung (IFU), Kreuzeckbahnstr. 19, D-82467 Garmisch-Partenkirchen, Germany. (trickl@ifu.fhg.de)

(Received December 31, 1998; revised July 16, 1999;
accepted July 27, 1999.)